PNAS
www.pnas.org

Supplementary Information for

Hinge point emergence in mammalian spinal neurulation

Veerle de Goederen, Roman Vetter, Katie McDole and Dagmar Iber

Dagmar Iber.
E-mail: dagmar.iber@bsse.ethz.ch

This PDF file includes:

Figs. S1 to S2
Tables S1 to S2
Legends for Movies S1 to S17

Other supplementary materials for this manuscript include the following:

Movies S1 to S17

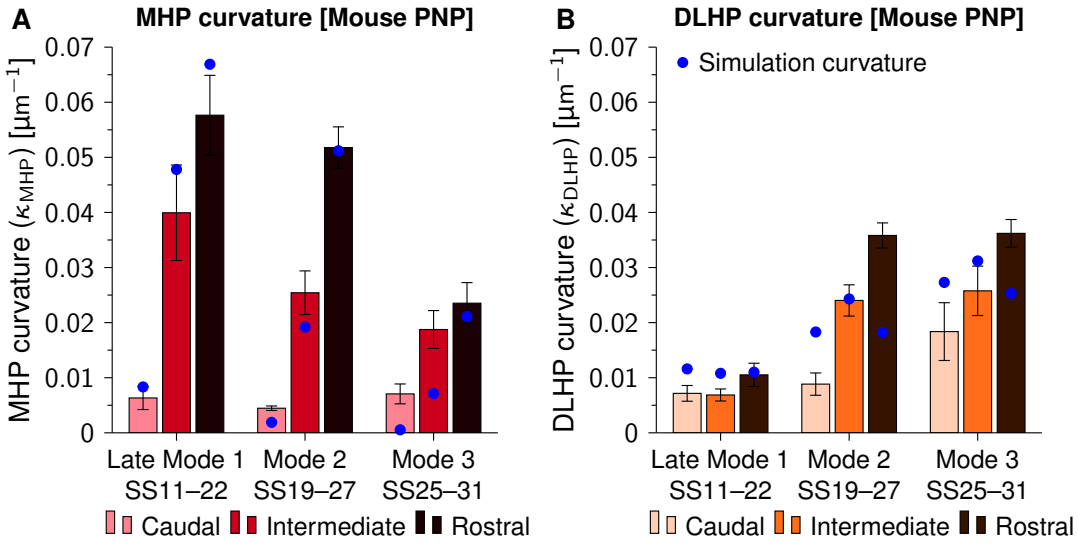

Fig. S1. Comparison of hinge point curvatures between experimental measurements and simulations. (A) Median hinge point curvature. (B) Dorsolateral hinge point curvature. Bars denote experimental quantifications in the mouse posterior neuropore (PNP); error bars are SEM from $N = 5, 12, 7$ measurements for folding modes 1–3. Blue dots are individual Model II simulations with midline thickness ratio $h_{\mathrm{NP}}/h_{\mathrm{HP}} = 1.5$ at mesoderm expansion factors $\alpha = 0.85, 0.45, 0.15$ (representing modes 1, 2, 3) at time points $t = 0.33, 0.66, 1$ (representing caudal, intermediate and rostral PNP positions). Curvature was measured as illustrated in Fig. S2E.

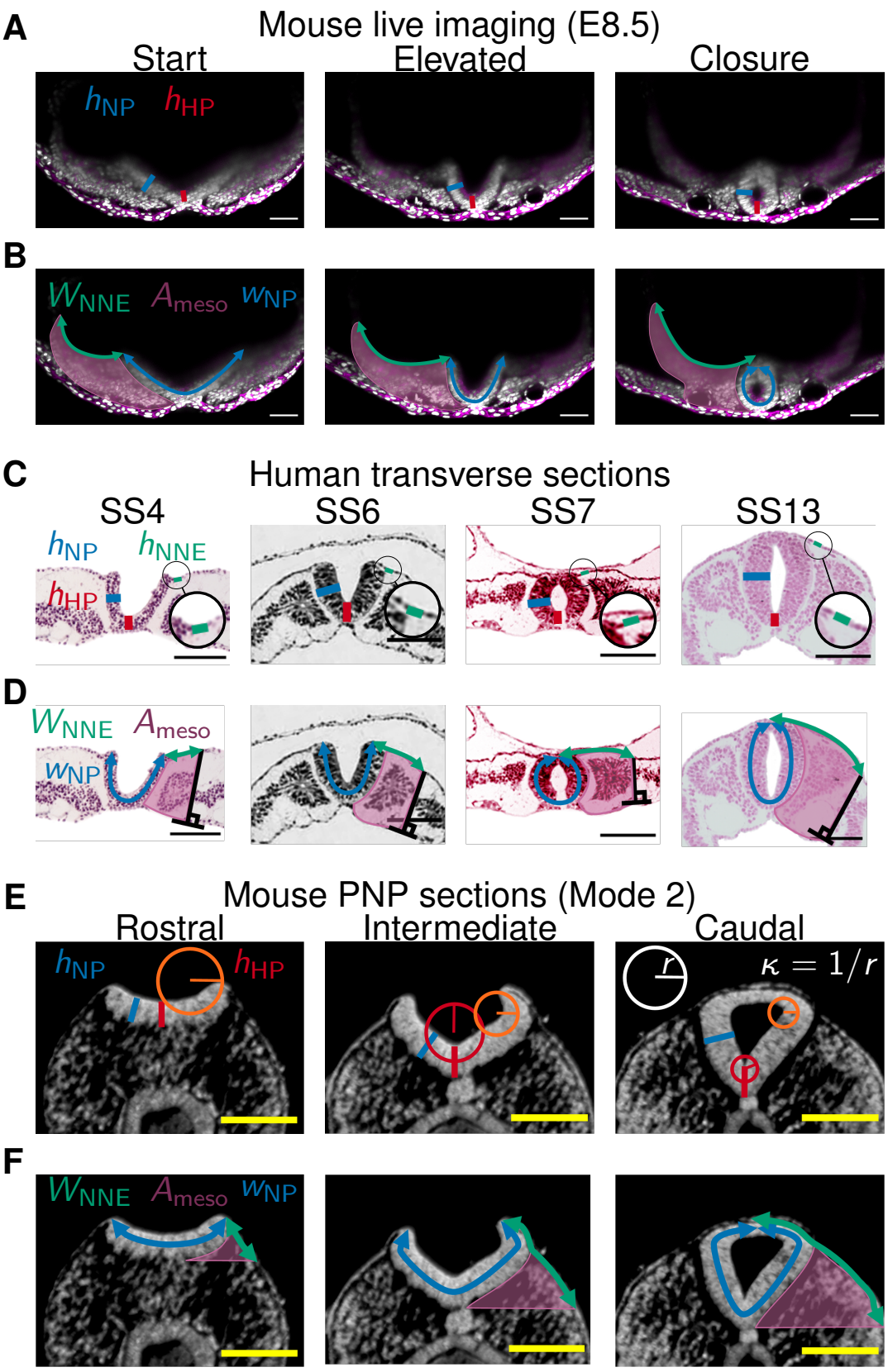

Fig. S2. Illustration of measurements performed in mouse live imaging data (A, B), human transverse sections (C, D) and mouse posterior neuropore data (E, F). (A, C, E) show neural plate height (h_{NP}, blue) and median hinge point height measurements (h_{HP}, red). (C) additionally shows NNE height (h_{NNE}, green, close-up circles) and (E) additionally shows the radius of curvature r of the median hinge point (red circles) and dorsolateral hinge point (orange circles). (B, D, F) show neural plate width (w_{NP}, blue), non-neural ectoderm width (w_{NP}, green) and mesoderm area (A_{meso}, pink). Scale bars: 100 µm.

Table S1. Mouse live imaging measurements per somite position and folding stage

Somite position	Folding stage	N
1	start	2
1	elevated	1
1	closure	1
2	start	3
2	elevated	2
2	closure	2
3	start	3
3	elevated	3
3	closure	3
4	start	3
4	elevated	3
4	closure	3
5	start	3
5	elevated	3
5	closure	3
6	start	3
6	elevated	3
6	closure	3
7	start	2
7	elevated	2
7	closure	2
8	start	2
8	elevated	1
8	closure	1

Table S2. Overview of mouse specimens used for posterior neuropore analysis

Origin	embryo ID	Somite stage (estimate)	Folding mode
EMAP	EMA:24	11	1
EMAP	EMA:27	17	1
DMDD	DMDD1835	20	1
EMAP	EMA:36	22	1
EMAP	EMA:37	22	1
DMDD	DMDD1834	19	2
DMDD	DMDD3544	20	2
EMAP	EMA:28	22	2
DMDD	DMDD3527	24	2
DMDD	DMDD3541	24	2
DMDD	DMDD3528	25	2
DMDD	DMDD3532	25	2
DMDD	DMDD3500	26	2
DMDD	DMDD3510	27	2
DMDD	DMDD3514	27	2
DMDD	DMDD3521	27	2
DMDD	DMDD3524	27	2
DMDD	DMDD3538	27	2
DMDD	DMDD3517	25	3
DMDD	DMDD3507	26	3
DMDD	DMDD3536	26	3
DMDD	DMDD3531	27	3
DMDD	DMDD3506	28	3
DMDD	DMDD1904	31	3
DMDD	DMDD1911	31	3

Movie S1. Model I simulation with basic model conditions.

Movie S2. Mouse live imaging of early neural tube closure at E8.5, somite position 4.5, transverse view. Magenta, cell membrane; white, nucleus.

Movie S3. Model I simulation with midline tapering ($h_{\mathrm{NP}}/h_{\mathrm{HP}} = 2$ and $w_{\mathrm{HP}} = 2h_{\mathrm{NP}}$).

Movie S4. Model I simulation with midline intrinsic curvature ($\kappa_{\mathrm{mid}} = \kappa_{\mathrm{max}}$ and $w_{\mathrm{HP}} = 2h_{\mathrm{NP}}$).

Movie S5. Model I simulation with dorsolateral intrinsic curvature ($\kappa_{\mathrm{mid}} = \kappa_{\mathrm{max}}/2$, $w_{\mathrm{HP}} = 2h_{\mathrm{NP}}$ and $d = 2h_{\mathrm{NP}}$).

Movie S6. Model I simulation combining midline tapering and midline intrinsic curvature ($h_{\mathrm{NP}}/h_{\mathrm{HP}} = 2$, $\kappa_{\mathrm{mid}} = \kappa_{\mathrm{max}}$ and $w_{\mathrm{HP}} = 2h_{\mathrm{NP}}$).

Movie S7. Model I simulation as in Movie S6 with a NNE thickness profile ($h_{\mathrm{NNE}} = 8$ µm, $w_{\mathrm{NNE}} = 125$ µm on both sides, $w_{\mathrm{NP}} = 250$ µm).

Movie S8. Model I simulation as in Movie S7 with differential width expansion. NNE expands in width while NP width stays constant. Final total tissue width is 1000 µm.

Movie S9. Model I simulation as in Movie S8 with NP border intrinsic outward curvature ($\kappa_{\mathrm{mid}} = -\kappa_{\mathrm{max}}$ and $w_{\mathrm{BHP}} = 2h_{\mathrm{NP}}$).

Movie S10. Model II simulation mimicking Closure 1 (concave initial configuration). Green, NNE; Blue, NP.

Movie S11. Model II simulation mimicking Closure 1 (concave initial configuration), with NP width decrease over time (convergent extension). Green, NNE; Blue, NP.

Movie S12. Model II simulation mimicking Closure 1 (concave initial configuration), without midline tapering. Green, NNE; Blue, NP.

Movie S13. Model II simulation mimicking folding in the posterior neuropore (flat initial configuration), without zippering, mesoderm area increase factor $\alpha = 1$. Green, NNE; Blue, NP.

Movie S14. Model II simulation mimicking folding in the posterior neuropore (flat initial configuration), without zippering, mesoderm area increase factor $\alpha = 1.75$. Green, NNE; Blue, NP.

Movie S15. Model II simulation mimicking folding in the posterior neuropore (flat initial configuration), with zippering, mesoderm area increase factor $\alpha = 1$ (Mode 1). Green, NNE; Blue, NP.

Movie S16. Model II simulation mimicking folding in the posterior neuropore (flat initial configuration), with zippering, mesoderm area increase factor $\alpha = 0.45$ (Mode 2). Green, NNE; Blue, NP.

Movie S17. Model II simulation mimicking folding in the posterior neuropore (flat initial configuration), with zippering, mesoderm area increase factor $\alpha = 0.15$ (Mode 3). Green, NNE; Blue, NP.